Electrospinning of Keratin/Poly(ethylene oxide) Blend Nanofibers

A. Aluigi,[1] A. Varesano,[1] A. Montarsolo,[1] C. Vineis,[1] F. Ferrero,[2] G. Mazzuchetti,[1] C. Tonin[1]

[1]*CNR-ISMAC, National Research Concil-Institute for Macromolecular Studies, C. so G. Pella, 16-13900 Biella, Italy*
[2]*Politecnico di Torino, Department of Materials Science and Chemical Engineering, C. so Duca degli Abruzzi, 24-10129 Torino, Italy*

Received 30 January 2006; accepted 6 October 2006
DOI 10.1002/app.25623
Published online in Wiley InterScience (www.interscience.wiley.com).

ABSTRACT: Research on the electrospinning of nanofibers has increased in recent years because of the number of potential applications in different areas, ranging from technical textiles (e.g., filters, composite reinforcements, and protective fabrics) to biomedical commodities and devices such as bandages, membranes, bioactive surfaces, and porous substrates for tissue engineering, for which biocompatible polymers play an essential role. In this work, wool keratin/poly(ethylene oxide) nanofibers were electrospun from aqueous solutions of polymer blends under different operating conditions. The filaments were characterized with scanning electron microscopy, Fourier transform infrared, and differential scanning calorimetry analyses and compared with films of the same materials produced via casting with the aim of investigating structural changes due to the electrospinning process. © 2007 Wiley Periodicals, Inc. J Appl Polym Sci 104: 863–870, 2007

Key words: blends; biopolymers; water-soluble polymers

INTRODUCTION

The process of polymer fiber formation within an electric field has been known since the 1930s.[1] This technique was named *electrostatic spinning* or *electrospinning* in the 1990s.[2,3] Electrospinning has been recently rediscovered because it is a simple and versatile method of producing ultrafine (<1 μm) polymer fibers.[4,5]

The basic setup for an electrospinning apparatus consists of three components: (1) a high-voltage generator, (2) a syringe with a metallic nozzle, and (3) a grounded collector.[4,5] The polymer solution is placed in the syringe and pushed out from the nozzle connected to the generator. When the jet starts, nanofibers are gathered in the form of a disordered, continuous filament on the collector.

The process is widely studied for producing porous membranes and nanostructured nonwovens for a wide range of applications in biomedicine,[4–6] including tissue-engineering scaffolds and medical implant devices,[7–11] bioactive surfaces and drug delivery systems,[12–14] and wound dressing,[11,15,16] because the electrospun mats, characterized by a small pore size, high porosity, three-dimensional features, and high surface-area-to-volume ratio, promote cell attachment, growth, and proliferation. Other possible applications of polymeric nanofibrous materials include, for example, technological textiles for filtration media,[17,18] composite reinforcements, and protective fabrics.[19,20]

Many works have dealt with the electrospinning of proteins,[21–23] but few have reported on keratin, although it is one of the most abundant proteins, being the major component of hair, feathers, wool, nails, and horns of mammals, reptiles, and birds. Moreover, the disposal of organic wastes such as wool-fiber byproducts from the textile industry, poor-quality raw wools not fit for spinning, and horns, nails, and feathers from butchery[24] involves complex environmental and economic aspects because the total amount of these materials has been estimated to be more than 3 million tons per year.[25]

The pooling and processing of keratin wastes would allow better exploitation of such a large amount of biomass. Protein hydrolysis derivatives (i.e., peptides or amino acids) currently find profitable applications in the cosmetic and detergency industries. Research is in progress on the extraction and purification of protein fractions with the aim of producing innovative biomaterials such as films and filaments suitable for novel large-scale uses in conventional fields (i.e., packaging, textiles, sanitation, and filtration) or high-tech applications in niche sectors, such as biotechnology and medical commodities and devices, for which biocompatibility is essential.

Regenerated keratin films degrade *in vitro* (by trypsin) and *in vivo* (subcutaneous embedding in mice),[26] and they well support fibroblast cell attachment and proliferation, so they are expected to be suitable for biomedical use.[27] In addition, it is known that kerati-

Correspondence to: C. Tonin (c.tonin@bi.ismac.cnr.it).
Contract grant sponsor: Cariplo Foundation through the project Fibre on Demand.

Journal of Applied Polymer Science, Vol. 104, 863–870 (2007)

nous materials can absorb toxic substances such as heavy-metal ions,[28–31] formaldehyde, and other hazardous volatile organic compounds, so possible applications can be envisaged also in water purification and air cleaning by active filtration.

Unfortunately, the poor mechanical properties of regenerated keratin hinder its processability and restrict its practical applications to blends with appropriate polymers with better structural properties. Our attempts to obtain filaments or films of pure regenerated keratin were indeed unsuccessful; moreover, the literature includes reports on the fabrication of regenerated keratin films[32] with crosslinking agents and the fabrication of composite nanofibers of regenerated silk fibroin blended with synthetic polymers such as poly(ethylene oxide) (PEO).[21]

PEO is an amphiphilic, water-soluble, and nondegradable polymer with good biocompatibility[33] and low toxicity.[34] This polymer is often used as an ideal model for the electrospinning process[35,36] because it can be electrospun without defects from aqueous solutions in a rather narrow range of conditions.

This article discusses the production and characterization of nanofibers produced by the electrospinning of pure PEO and 50 : 50 (w/w) keratin/PEO blends from aqueous solutions of the polymers under different operating conditions. The nanofibers were studied with scanning electron microscopy (SEM), Fourier transform infrared (FTIR) spectroscopy, and differential scanning calorimetry (DSC). The results are compared with those obtained by thin films produced via casting from the same solutions with the aim of investigating the influence of the production processes on the structural arrangement of these materials.

EXPERIMENTAL

Materials

Keratin was obtained from wool by means of a sulfitolysis extraction method. The wool fibers were cleaned by Soxhlet extraction with petroleum ether to remove fatty matters, washed with distilled water, and conditioned at 20°C and 65% relative humidity for at least 24 h. The cleaned and conditioned fibers (3 g) were cut and placed in 100 mL of an aqueous solution containing urea (8*M*), *m*-bisulfite (0.5*M*), and sodium dodecyl sulfate (SDS, 0.05*M*), which was adjusted to pH 6.5 with 5*N* NaOH. The mixture was heated to 65°C and shaken for 5 h. After that, it was filtered through a stainless steel mesh (50 mesh) and dialyzed (with a cellulose tube with a molecular weight cutoff of 12,000–14,000 Da) against distilled water for 3 days. The insoluble material was removed by centrifugation on a centrifugally driven Millipore filter (5-μm pore size) for 15 min at 12,000 rpm (Millipore Corp., Redford, MA). The keratin concentration was measured by the Bradford protein assay method (with bovine serum albumin as a standard).[37] The solution was concentrated to 2.5, 3.5, and 5.0 wt % in a Buchi Rotavapor R-205 rotary vacuum evaporator (Buchi Labortech GmbH, Postfach, Switzerland).

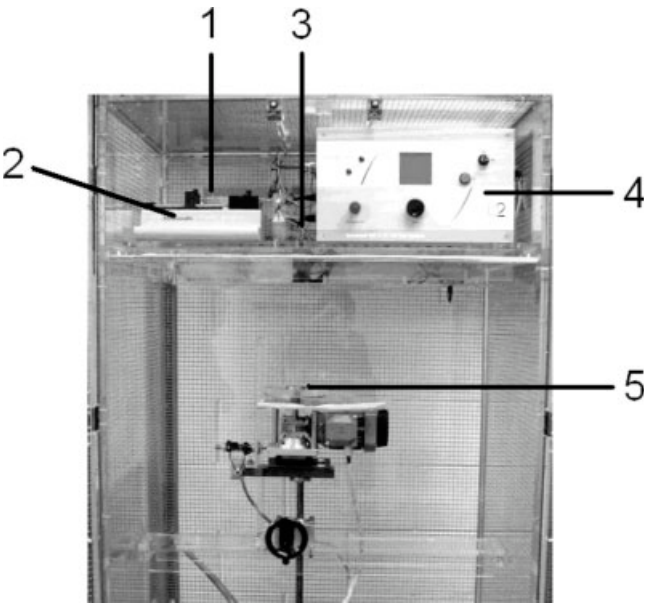

Figure 1 Picture of the electrospinning device: (1) syringe, (2) metering pump, (3) capillary with a metal tip, (4) high-voltage generator, and (5) collector (metal disk).

PEO powder with a viscosity-average molecular weight of 4×10^5 g/mol (from Sigma–Aldrich, St. Louis, MO) was dissolved in distilled water at the ambient temperature for about 12 h. The concentrations were 5, 7, and 10 wt %.

The keratin/PEO blend solutions were prepared at room temperature in about 12 h by the simple addition of PEO powder to the keratin aqueous solution. The solutions of the keratin/PEO blend had total polymer concentrations of 5, 7, and 10 wt % with a keratin/PEO weight ratio of 50 : 50.

Electrospinning

The electrospinning device assembled in our laboratory (Fig. 1) consisted of a syringe pushed with an automatic metering pump (KDS200, KD Scientific, Holliston, MA). The syringe was linked to a capillary pipe with a metallic tip (internal diameter of 0.20 mm and length of ca. 3 cm) electrically connected to a high-voltage generator (HVA b2 Electronics, GmbH, Klaus, Austria). The generator and the metering pump were controlled by a remote personal computer. The grounded collector was a rotating, stainless steel disk 5.5 cm in diameter covered with an aluminum sheet to prevent damage due to the following manipulations for the sample testing.

The process started when the electrostatic forces acting on the pendent drop of the solution at the capillary

TABLE I
Conductivity Measurements of the Polymer Solutions

Polymer concentration (wt %)	Conductivity (mS/cm)	
	Pure PEO	50 : 50 keratin/PEO
5	0.123	1.042
7	0.120	1.282
10	0.119	1.644

tip overcame the solution surface tension, the drop was deformed into a conical shape called a Taylor cone, and a jet was ejected and accelerated toward the grounded collector by the electrical field. While traveling from the nozzle to the collector, the jet was subjected to a whipping instability that caused bending and stretching of the jet. As the solvent evaporated, filaments of the polymer solidified and deposited themselves on the collector as a disordered, nanostructured mat.

The solutions of PEO and 50:50 keratin/PEO at 5, 7, and 10 wt % concentrations of the polymers in water were electrospun at a 20-cm working distance to ensure that the nanofibers were dried. The applied voltages were between 10 and 30 kV. About 5 mL of the polymer solution was placed in the syringe. The tip was positively charged by the generator. When a steady voltage was reached between the tip and collector, the delivery pump switched on and fed the fixed flow of the solution through the capillary, and the electrospinning process started. The process was stopped after about 10 min. During the electrospinning process, environmental conditions were kept in check; in particular, the temperature was ranged from 20 to 25°C, and the relative humidity was in the range of 55–65%.

Analyses and characterization

The conductivity of the polymer solutions was measured with a Eutech Instruments PC300 multiparameter tester (Eutech Instruments Europe B.V., Nijkark, The Netherlands). Before its use, the conductivity tester was calibrated by a 1.413 mS/cm (at 25°C) standard solution. The conductivities are reported in millisiemens per centimeter.

The viscosity measurements were carried out in an Anton Paar Physica MCR 301 rheometer (Anton Paar GmbH, Graz, Austria) equipped with a PTD 200 Peltier temperature-control device at 25.0 ± 0.1°C with cone–plate geometry (75-mm diameter, 1° angle, and 45-μm truncation). The shear rate was logarithmically increased from 0.1 to 10,000 s^{-1}. Data were acquired and elaborated with Rheoplus (Anton Paar GmbH, Grax, Austria) version 2.66 software.

The SEM investigation was performed with a Leica Electron Optics 135 VP SEM instrument (LEO Electron Microscopy Ltd., Cambridge, UK) at an acceleration voltage of 15 kV, with a 50-pA current probe, and at a working distance of about 20 mm. An aluminum sheet with the nanofiber mat was cut and mounted on aluminum specimen stubs with double-sided adhesive tape. The samples were sputter-coated with a gold layer in rarefied argon with an Emitech K550 sputter coater (EM Technologies Ltd., Kent, UK) with a current of 20 mA for 180 s.

The diameters of the electrospun nanofibers were measured (with Opera Plus version 6.12 software by MAD Software GmbH, Austria) from SEM pictures randomly collected from the samples. For each sample, the average value and its standard deviation were calculated from 150 measured diameters.

FTIR spectra were acquired with a Thermo Nicolet (Madison, WI) Nexus spectrometer by the attenuated-total-reflection technique with a Smart Endurance accessory from 4000 to 600 cm^{-1} with 100 scansions, a 4-cm^{-1} band resolution, and a gain of 8.0.

DSC was performed with a Mettler–Toledo DSC 821 (Schwcrzenbach, Switzerland) calibrated by an indium standard. The calorimeter cell was flushed with 100 mL/min nitrogen. About 3 mg of the sample was used in each test with aluminum crucibles. The runs were performed from 30 to 400°C at a heating rate of 10°C/min. The data were collected on a computer with the Mettler–Toledo STARe system.

RESULTS AND DISCUSSION

Solution characterization

The viscosity is an important factor for complete fiber formation in the electrospinning of polymer solutions. In particular, fibers without beads are produced when polymer chain entanglements are present.[38] Moreover, fiber formation is promoted at low polymer concentrations, which increase the solution conductivity.[39]

The conductivities of the solutions are reported in Table I. A great increase in the conductivity was measured from solutions containing keratin because of SDS that remained associated with keratin through ionic interactions conferring negative charges to the protein.[40]

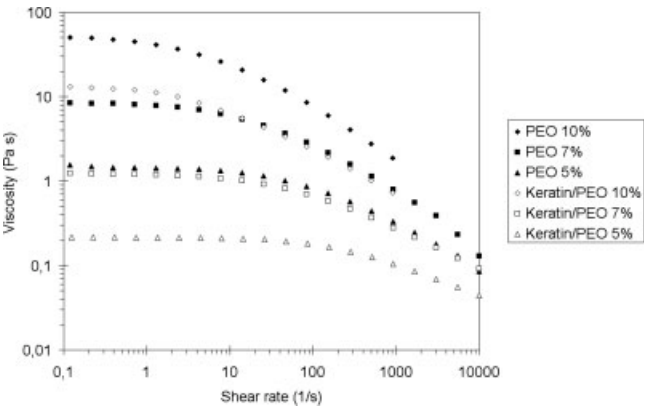

Figure 2 Viscosity flow curves of PEO and keratin/PEO solutions.

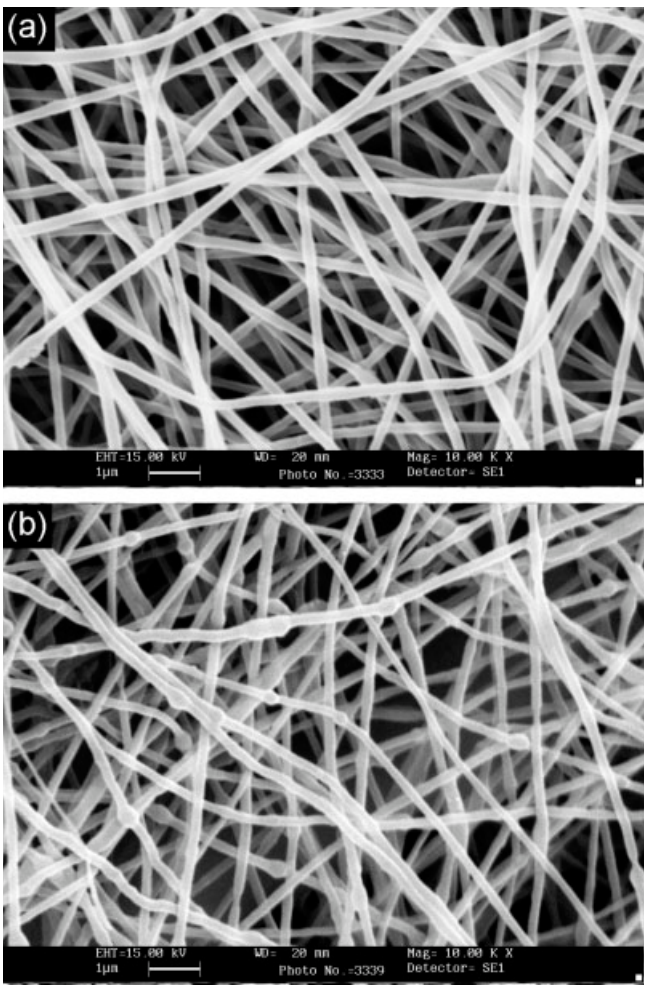

Figure 3 Electrospun nanofibers from 7 wt % solutions of pure PEO in water: (a) 20 kV and 0.01 mL/min (10,000×) and (b) 30 kV and 0.03 mL/min (10,000×).

Flow curves (viscosity vs shear rate) of PEO and 50 : 50 keratin/PEO solutions with 5, 7, and 10 wt % polymer in water are reported in Figure 2. All solutions behave like shear-thinning fluids. At low shear rates, disentanglement is balanced by the formation of new entanglements, so the fluid has a Newtonian behavior that corresponds to a constant viscosity value (zero-shear viscosity). At higher values of the shear rate, the disentanglement rate exceeds the rate of entanglement formation; therefore, the viscosity decreases and shear-thinning behavior can be observed. The onset of shear thinning (corresponding to the transition from Newtonian behavior to shear-thinning behavior) shifts to lower values of the shear rate with an increase in the polymer concentrations for both pure PEO and keratin/PEO solutions. The zero-shear viscosity, estimated from the flow curve, increases when the polymer concentration increases. The keratin/PEO solutions at concentrations of 7 and 10 wt % show flow curves to 5 and 7% PEO solutions, respectively. Thus, keratin with a relatively low molecular weight slightly increases the viscosities of the keratin/PEO solutions, but its contribution is not negligible.

Morphology

The morphologies of the electrospun materials were investigated through the SEM analysis of samples pro-

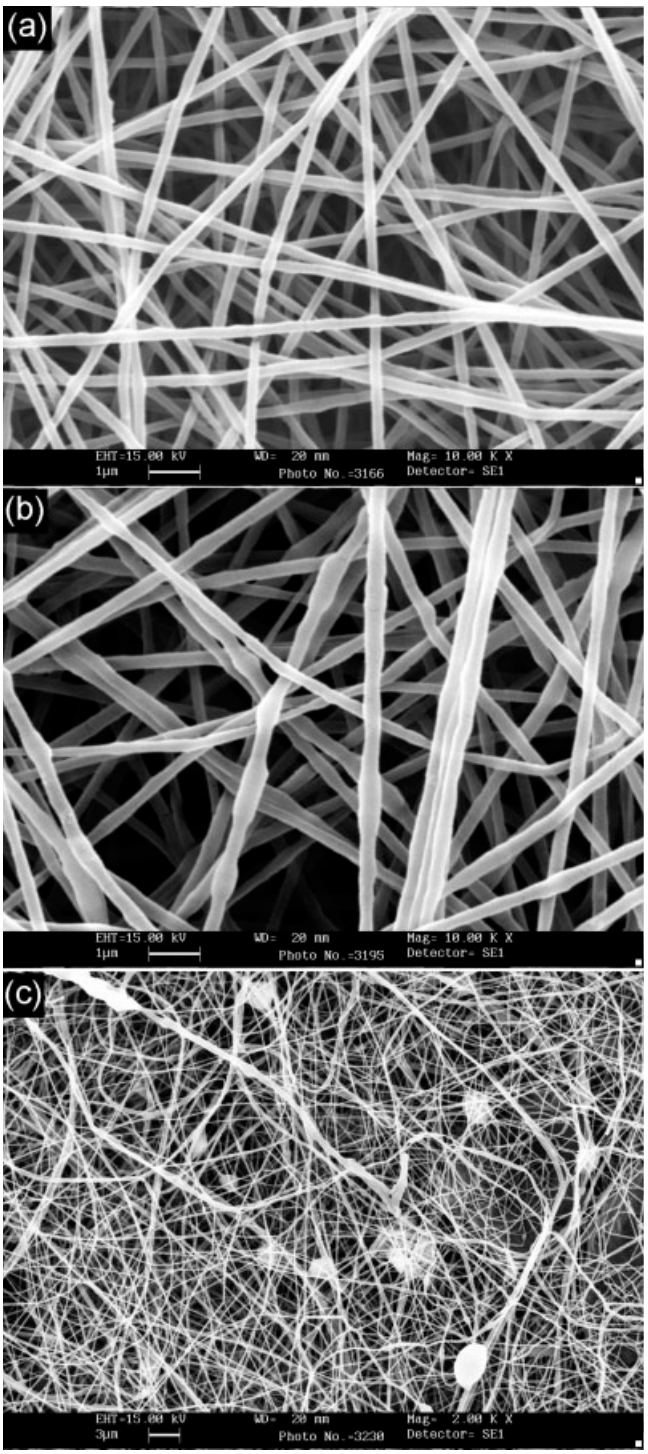

Figure 4 Electrospun nanofibers from 5 wt % solutions of pure PEO in water: (a) 15 kV and 0.01 mL/min (10,000×), (b) 20 kV and 0.03 mL/min (10,000×), and (c) 30 kV and 0.05 mL/min (2000×).

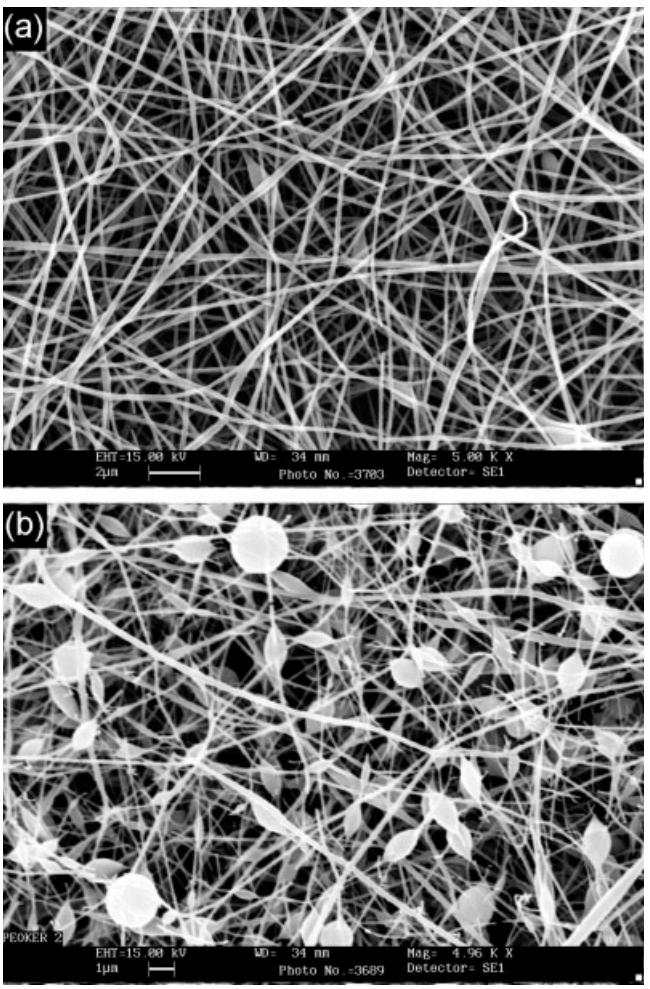

Figure 5 Electrospun nanofibers of 50:50 keratin/PEO blends at 25 kV and 0.01 mL/min from (a) 7 wt % (5000×) and (b) 5 wt % (4960×) solutions in water.

duced with various flow rates, voltages, and concentrations of PEO solutions at a 20-cm working distance.

Nanofibers without defects were produced from the 7 wt % solution at a 0.01 mL/min flow rate from 20 to 30 kV, as shown in Figure 3(a). As the flow rate increased up to 0.03 mL/min, the 30-kV voltage became insufficient to completely draw the jet, and the nanofibers appeared to be more irregular with some nanoscopic defects (beads) with diameters less than 400 nm, as shown in Figure 3(b). For a higher flow rate (0.05 mL/min), macroscopic drops fell from the capillary also at the highest voltage (30 kV).

The electrospinning of a 5 wt % solution produced nanofibers without defects with a flow rate of 0.01 mL/min within a voltage range of 13–30 kV [see Fig. 4(a)]. Nevertheless, at 13 kV, some drops fell from the capillary because the flow rate of the jet was lower than the delivered one. When the flow rate was increased to 0.03 mL/min, the nanofibers became more irregular with some beads because of the insufficient stretching of the jet at voltages below 25 kV, as shown in Figure 4(b). For a higher flow rate (0.05 mL/min), the process started only at a 30-kV voltage, whereas at a lower voltage, the solution dripped from the capillary, and drops were observed [see Fig. 4(c)].

Nanofibers of a 50 : 50 keratin/PEO blend with a regular diameter distribution and few defects were electrospun from solutions with 7 and 10 wt % polymer concentrations with a voltage of 20–30 kV and a solution flow rate of 0.01 mL/min [see Fig. 5(a)]. The keratin/PEO solutions at high concentrations (7 and 10 wt %) produced fibers with few defects, like 5 and 7% PEO solutions, probably because they had a similar flow behavior, as shown in Figure 2. At a low polymer concentration (5 wt %), the nanofibers were electrospun with many defects also at a high voltage (25–30 kV), as Figure 5(b) shows, and the solution dripped from the capillary during the process at a voltage below 20 kV because of the low viscosity (see Fig. 2).

The diameters of the filaments were measured at 150 different points from SEM pictures for each sample produced. Figure 6 shows the average diameter of the electrospun nanofibers as a function of the applied voltage. The flow rate and the working distance were held constant at 0.01 mL/min and 20 cm, respectively. As the voltages increased, the diameters of the nanofibers obtained from all the solutions decreased. As shown by the trend lines, the diameters of the nanofibers produced at the same voltage from 5 and 7 wt % pure PEO solutions were generally comparable. The keratin/PEO solution produced nanofibers with a small diameter at a higher voltage (30 kV), whereas at 20 kV, the electrospun nanofibers had a diameter much higher than the pure PEO nanofibers at the same voltage. Moreover, the slope of the diameter/voltage trend line for the keratin/PEO blend was the highest obtained in our experiment.

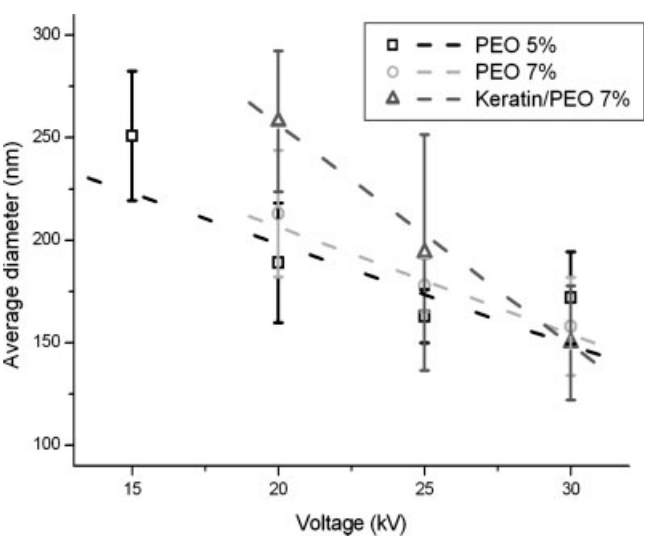

Figure 6 Average diameters of electrospun nanofibers as a function of the applied voltage.

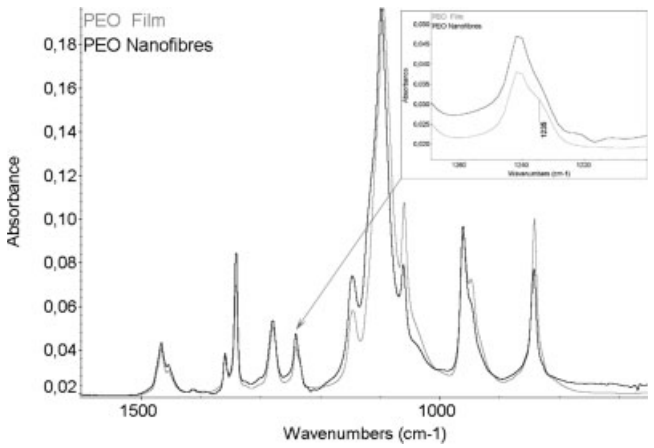

Figure 7 FTIR spectra of a PEO film from casting and PEO nanofibers from electrospinning.

Thus, it seems that the presence of keratin strengthens the influence of the voltage on the size of the filaments. Because keratin has many different functional groups, it is possible that inter- and intramolecular bonds (i.e., hydrogen bonds, ionic interactions, and van der Waals forces) increase the jet rigidity when the solvent evaporates. Therefore, a higher voltage is required to stretch the solidifying keratin/PEO solution jet.

IR analysis

The FTIR spectra of keratin and PEO present absorptions in the region below 2000 cm^{-1} with several overlapped bands, except for the amide I band (1750–1580 cm^{-1}) of keratin and the C—O—C stretching of PEO, which fall in the range of 1150–1050 cm^{-1}. FTIR analysis shows that nanofibers with and without defects had the same spectral features (the spectra are not reported here for the sake of brevity).

FTIR spectra of electrospun samples were compared with the spectra of the films produced via casting from the same solution, with the aim of highlighting the structural changes induced by the electrospinning process. Figure 7 shows FTIR spectra of a pure PEO film and PEO nanofibers in the range of 1200–900 cm^{-1}. The presence of the crystalline PEO phase is confirmed by the triplet peak of the C—O—C stretching vibration at 1145, 1094, and 1060 cm^{-1}, with the highest absorption at 1094 cm^{-1}. Changes in the intensity, shape, and position of the C—O—C stretching absorptions indicate changes in the conformational structures, as reported by Deitzel et al.[41] The intensities of the peaks at 1145 and 1240 cm^{-1} are due to the planar conformation increase in the electrospun samples, whereas the peaks related to the helical conformation at 1060, 947, and 841 cm^{-1} decrease. Moreover, the shoulder at 1235 cm^{-1}, assigned to the helical conformation and observed in the PEO film spectrum, disappears for the relative electrospun sample.[42,43] These results suggest that the electrospinning process promotes the planar conformation of PEO.

The amide I band of keratin originates primarily from the C=O stretching vibration and is widely used to study the protein secondary structure. In fact, the frequency of C=O stretching is due to the backbone conformation and the hydrogen-bonding pattern, so it depends on the chemical surroundings of the carbonyl groups. Regenerated keratin from wool is a biological polymer characterized by a wide distribution of molecular weights and heterogeneous supermolecular structures; thus, the amide I band consists of several overlapping bands related to different chain arrangements. The amide I band in the keratin/PEO blend film (reported in Fig. 8) shows a doublet peak at 1650 and 1624 cm^{-1}, which indicates different keratin structures. In the relative electrospun sample, the amide I band assumes a symmetric shape centered at 1650 cm^{-1}. It is known that the frequency of the C=O vibration is related to the strength of the hydrogen bond formed: stronger hydrogen bonds correspond to lower frequencies of amide I.[44] Therefore, the presence of the single absorption band at higher wave numbers suggests that the electrospinning process promotes the molecular orientation of the keratin chains in which the carbonyl groups are involved in weaker hydrogen bonds.

Calorimetric analysis

The DSC curves of keratin/PEO samples (films and nanofibers) are shown in Figure 9. The endothermic overlapped peaks around 60°C are due to the fusion of the PEO crystalline phase and to the evaporation of

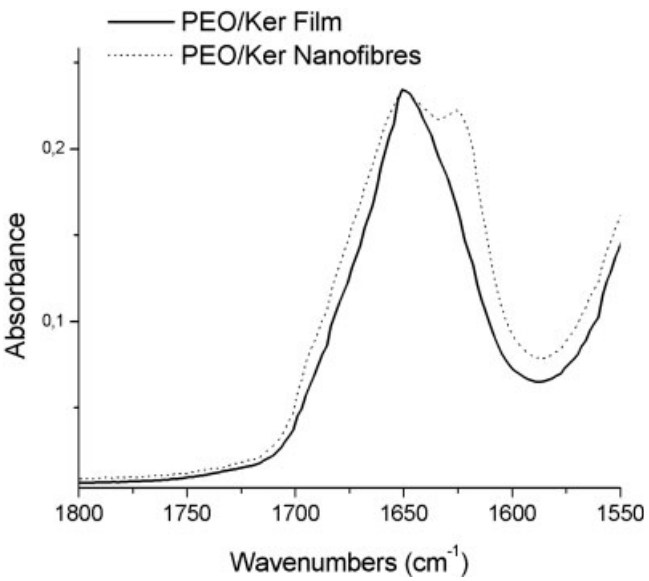

Figure 8 FTIR spectra of a keratin/PEO film from casting and keratin/PEO nanofibers from electrospinning.

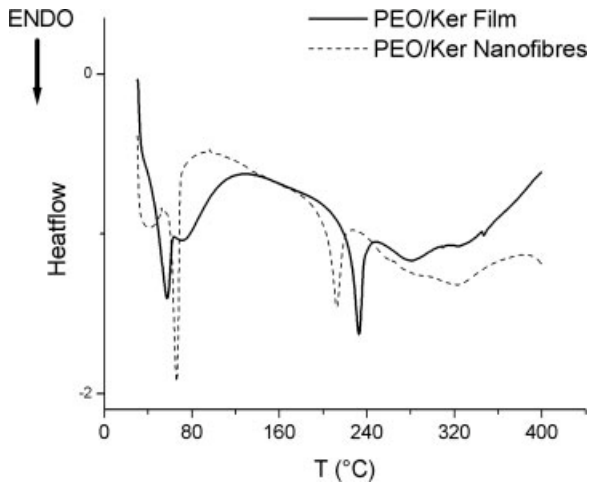

Figure 9 DSC analysis of a keratin/PEO film from casting and keratin/PEO nanofibers from electrospinning.

water, especially that absorbed by keratin. In the keratin/PEO film, water evaporation occurs at a lower temperature with respect to keratin/PEO nanofibers (ca. 50°C in the nanofibers and ca. 80°C in the film). This is probably due to the high surface/volume ratio of the nanofibers, which promotes water evaporation even at lower temperatures. In agreement with the DSC analysis of Kim et al.,[43] the electrospun PEO exhibits a slight increase in the melting point. It is believed that the high stretching due to the electrospinning process promotes the orientation of the long polymer chains of PEO. This high degree of order shifts the melting point to a higher temperature. Therefore, the electrospinning process changes both the conformation (see FTIR analysis) and thermal behavior of the polymer.

The endothermic events observed in the range of 200–350°C are attributed to protein denaturation followed by protein degradation.[45] The thermograms show that the peaks related to the protein denaturation, which falls at 233°C in the film, shift to a lower temperature (213°C) in the electrospun sample. It could be presumed that the high draw, given by the electrospinning process, and the quick water evaporation hinder the keratin self-assembly, leading the protein chains to assume a less complex supermolecular organization that denatures at lower temperatures. This thermal behavior is in agreement with the FTIR observations; in fact, the keratin in the electrospun fibers shows a molecular conformation characterized by weaker hydrogen bonds that make the protein less thermally stable.

CONCLUSIONS

SEM investigations of electrospun materials produced from PEO and keratin/PEO aqueous solutions have provided us information to determine the electrospinning process parameters to make membranes free of defects. 50:50 keratin/PEO solutions with 7 and 10 wt % polymer concentrations have sufficient viscosity to be electrospun with few defects. The measurements of the fiber diameters shows that the production of keratin/PEO nanofibers is more strongly influenced by the applied voltage than the pure PEO nanofibers. FTIR analysis indicates that the pure PEO electrospun fibers have a crystalline microstructure with a more developed planar conformation with respect to the helical conformation. Spectroscopic and thermal analysis of the keratin/PEO blend nanofibers indicates that the electrospinning process hinders the natural self-assembly of *S*-sulfo keratin, leading to the formation of a less complex protein conformation. Details about the polymer interactions, crystallization, and mechanical properties of the new material are open to specific investigation.

The electrospinning apparatus was acquired by the Laboratorio di Alta Tecnologia Tessile of CNR-ISMAC National Research Concil-Institute for Macromolecular Studies Biella with the sponsorship of the Regione Piemonte.

References

1. Formhals, A. U.S. Pat. 1,975,504 (1934).
2. Doshi, J.; Reneker, D. H. Proc IEEE Ind Appl Soc Meeting 1993, 3, 1698.
3. Doshi, J.; Reneker, D. H. J Electrostatics 1995, 35, 151.
4. Li, D.; Xia, Y. Adv Mater 2004, 16, 1151.
5. Subbiah, T.; Bhat, G. S.; Tock, R. W.; Parameswaran, S.; Ramkumar, S. S. J Appl Polym Sci 2005, 96, 557.
6. Frenot, A.; Chronakis, I. S. Curr Opin Colloid Interface Sci 2003, 8, 64.
7. Ma, Z.; Kotaki, M.; Inai, R.; Ramakrishna, S. Tissue Eng 2005, 11, 101.
8. Huang, L.; Nagapudi, K.; Apkarian, R. P.; Chaikof, E. L. J Biomater Sci Polym Ed 2001, 12, 979.
9. Matthews, J. A.; Wnek, G. E.; Simpson, D. G.; Bowlin, G. L. Biomacromolecules 2002, 3, 232.
10. Li, W. J.; Laurencin, C. T.; Caterson, E. J.; Tuan, R. S.; Ko, F. K. J Biomed Mater Res 2002, 60, 613.
11. Min, B. M.; Lee, G.; Kim, S. H.; Nam, Y. S.; Lee, T. S.; Park, W. H. Biomaterials 2004, 25, 1289.
12. Kenawy, E. R.; Bowlin, G. L.; Mansfield, K.; Layman, J.; Simpson, D. G.; Sanders, E. H.; Wnek, G. E. J Controlled Release 2002, 81, 57.
13. Kim, K.; Luu, Y. K.; Chang, C.; Fang, D.; Hsiao, B. S.; Chu, B.; Hadjiargyrou, M. J Controlled Release 2004, 98, 47.
14. Zeng, J.; Yang, L.; Liang, Q.; Zhang, X.; Guan, H.; Xu, X.; Chen, X.; Jing, X. J Controlled Release 2005, 105, 43.
15. Kenawy, E. R.; Layman, J. M.; Watkins, J. R.; Bowlin, G. L.; Matthews, J. A.; Simpson, D. G.; Wnek, G. E. Biomaterials 2003, 24, 907.
16. Casper, C. L.; Yamaguchi, N.; Kiick, K. L.; Rabolt, J. F. Biomacromolecules 2005, 6, 1998.
17. Tsai, P. P.; Schreuder-Gibson, H.; Gibson, P. J Electrostatics 2002, 54, 333.
18. Graham, K.; Ouyang, M.; Raether, T.; Grafe, T.; McDonald, B.; Knauf, P. Presented at the 15th Annual Technical Conference and Expo of the American Filtration and Separations Society, Galveston, TX, April 9–12, 2002.

19. Schreuder-Gibson, H.; Gibson, P.; Senecal, K.; Sennett, M.; Walker, J.; Yeomans, W.; Ziegler, D.; Tsai, P. P. J Adv Mater 2002, 34, 44.
20. Kim, J. S.; Reneker, D. H. Polym Compos 1999, 20, 124.
21. Jin, H. J.; Fridrikh, S. V.; Rutledge, G. C.; Kaplan, D. L. Biomacromolecules 2002, 3, 1233.
22. Nagapudi, K.; Brinkman, W. T.; Leisen, J. E.; Huang, L.; McMillan, R. A.; Apkarian, R. P.; Conticello, V. P.; Chaikof, E. L. Macromolecules 2002, 35, 1730.
23. Xie, J. B.; Hsieh, Y. L. J Mater Sci 2003, 38, 2125.
24. Salminen, E.; Rintala, J. Bioresour Technol 2002, 83, 13.
25. Moncrieff, R. W. Man Made Fibres, 6th ed.; Butterworths Scientific: London, 1975; Vol. 11, p 231.
26. Yamauchi, K.; Yamauchi, A.; Kusunoki, T.; Kohda, A.; Konishi, Y. J Biomed Mater Res 1996, 31, 439.
27. Yamauchi, K.; Maniwa, M.; Mori, T. J Biomater Sci Polym Ed 1998, 9, 259.
28. Kar, P.; Misra, M. J Chem Technol Biotechnol 2004, 79, 1313.
29. Kokot, S. Text Res J 1993, 63, 159.
30. Masri, S. M.; Friedman, M. Adv Exp Med Biol 1974, 48, 551.
31. Hartley, F. R. Aust J Chem 1968, 21, 1013.
32. Tanabe, T.; Okitsu, N.; Yamauchi, K. Mater Sci Eng C 2004, 24, 441.
33. Desai, N. P.; Hubbel, J. A. Biomaterials 1991, 12, 144.
34. Bergsma, J. E.; Rozema, F. R.; Bos, R. R. M.; de Bruijn, W. C.; Boering, G.; Pennings, A. J. Biomaterials 1995, 16, 267.
35. Theron, S. A.; Zussman, E.; Yarin, A. L. Polymer 2004, 45, 2017.
36. Son, W. K.; Youk, J. H.; Lee, T. S.; Park, W. H. Polymer 2004, 45, 2959.
37. Bradford, M. Anal Biochem 1976, 72, 248.
38. Shenoy, S. L.; Bates, W. D.; Frisch, H. L.; Wnek, G. E. Polymer 2005, 46, 3372.
39. Son, W. K.; Youk, J. H.; Lee, T. S.; Park, W. H. Polymer 2004, 45, 2959.
40. Schrooyen, P. M. M.; Dijkstra, P. J.; Oberthür, R. C.; Bantjes, A.; Feijen, J. J Colloid Interface Sci 2001, 240, 30.
41. Deitzel, J. M.; Kleinmeyer, J. D.; Hirvonen, J. K.; Beck Tan, N. C. Polymer 2001, 42, 8163.
42. Barthet, C.; Guglielmi, M.; Baudry, P. J Electroanal Chem 1997, 431, 145.
43. Kim, G. M.; Wutzier, A.; Radusch, H. J.; Michler, G. H.; Simon, P.; Sperling, R. A.; Parak, W. J. Chem Mater 2005, 17, 4949.
44. Gribenow, K.; Santos, A. M.; Carrasquillo, K. G. Internet J Vib Spectrosc 1999, 3, 1.
45. Spei, M.; Holzem, R. Colloid Polym Sci 1990, 268, 630.